Natural compounds as angiogenic enzyme thymidine phosphorylase inhibitors: *In vitro* biochemical inhibition, mechanistic, and *in silico* modeling studies
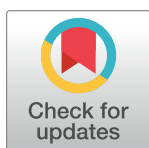
Sumaira Javaid[1☯]**, Muniza Shaikh**[1☯]**, Narjis Fatima**[1‡]**, M. Iqbal Choudhary**[1,2,3‡]*

1 Dr. Panjwani Center for Molecular Medicine and Drug Research, International Center of Chemical and Biological Sciences, University of Karachi, Karachi, Pakistan, **2** H. E. J. Research Institute of Chemistry, International Center for Chemical and Biological Sciences, University of Karachi, Karachi, Pakistan, **3** Department of Biochemistry, Faculty of Sciences, King Abdulaziz University, Jeddah, Saudi Arabia

☯ These authors contributed equally to this work.
‡ These authors also contributed equally to this work.
* iqbal.choudhary@iccs.edu

Abstract

Natural flora is the richest source of novel therapeutic agents due to their immense chemical diversity and novel biological properties. In this regard, eighteen natural products belonging to different chemical classes were evaluated for their thymidine phosphorylase (TP) inhibitory activity. TP shares identity with an angiogenic protein platelet derived endothelial cell growth factor (PD-ECGF). It assists tumor angiogenesis and is a key player in cancer progression, thus an ideal target to develop anti-angiogenic drugs. Eleven compounds **1**–**2**, **5**–**10**, **11**, **15**, and **18** showed a good to weak TP inhibitory activity (IC_{50} values between 44.0 to 420.3 μM), as compared to standards *i.e.* tipiracil (IC_{50} = 0.014 ± 0.002 μM) and 7-deazaxanthine (IC_{50} = 41.0 ± 1.63 μM). Kinetic studies were also performed on active compounds, in order to deduce the mechanism of ligand binding to enzyme. To get further insight into receptor protein (enzyme) and ligand interaction at atomic level, *in-sillico* studies were also performed. Active compounds were finally evaluated for cytotoxicity test against mouse fibroblast (3T3) cell line. Compound **18** (Masoprocol) showed a significant TP inhibitory activity (IC_{50} = 44.0 ± 0.5 μM). Kinetic studies showed that it inhibits the enzyme in a competitive manner (K_i = 25.6 ± 0.008 μM), while it adopts a binding pose different than the substrate thymidine. It is further found to be non-toxic in MTT cytotoxicity assay. This is the first report on TP inhibitory activity of several natural compounds, some of which may serve as leads for further research towards drug the development.

Introduction

Cancer is one of the primary causes of death worldwide, with approximately one in six person dies because of some malignant conditions. In the last few decades, early diagnosis and treatment have improved the patient's life quality, and survival rates. However, there are still high rates of recurrence, invasiveness, and metastases. To improve efficacy, new therapeutic

interventions are required which target different and important stages of tumor progression. In this context, angiogenesis has emerged as a hallmark of tumor growth. Since the last five decades, it has been hypothesized that blocking angiogenesis could be an effective way to combat the disease's progression. Thenceforth, a large number of molecules, targeting the process of angiogenesis, have been under pre-clinical and clinical trials. Some of these molecules are already approved as drugs by the U.S. Food and Drug Administration (FDA). Thymidine phosphorylase (TP) is among the several factors that stimulate the growth of blood vessels, and it described as a validated target for the antiangiogenic compounds development [1].

Enzyme thymidine phosphorylase (TP) is involved in pyrimidine salvage pathway, regulating the nucleotide homeostasis which is required for DNA repair and replication. It catalyzes the reversible phosphorolysis of thymidine to thymine and 2-deoxyribose-1-phosphate. 2-Deoxyribose-1-phosphate then undergoes dephosphorylation to 2-deoxyribose, which actually triggers tumor angiogenesis. 2-Deoxyribose affects endothelial-cell migration by activating the downstream integrin signaling pathway. It also augment the expression and/or release of several angiogenic growth factors, such as VEGF, MMPs, cytokines, interleukins, and others, which in the tumor microenvironment enhance the angiogenesis, and cancer metastasis. TP is reported to share sequence homology with an angiogenic growth factor (Platelet derived endothelial cell growth factor; PD-ECGF), which promotes angiogenesis by facilitating endothelial cells proliferation, and migration [2, 3].
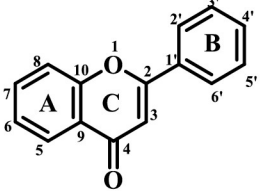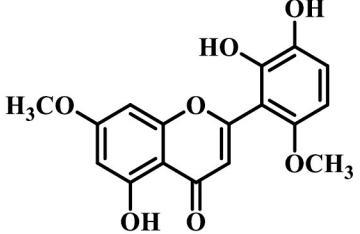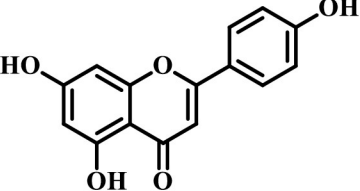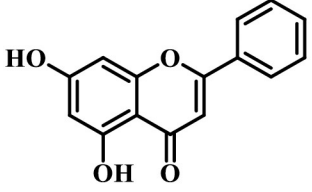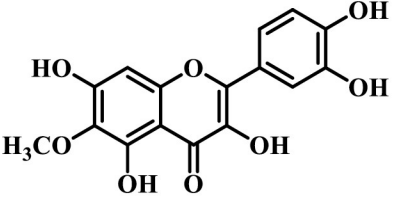
Over-expression of TP has been associated with cancer aggressiveness, and poor prognosis. Different solid tumors, including breast, colorectal, bladder, and esophageal cancers are being reported with high levels of TP [4–7]. In addition to this some other diseases, such as rheumatoid arthritis, psoriasis, and inflammation also show high levels of TP activity [8]. Several TP inhibitors have been reported with potent activities *in vitro*, however, only one TP inhibitor (tipiracil) in combination of a cytotoxin (trifluridine) is US-FDA approved for the management of colorectal cancer. Usage of this combination drug (Lonsruf) is compromised with several side effects, such as neutropenia, anemia, myelosuppression, etc [9–20].

Our research group has previously reported several synthetic and few natural inhibitors of TP [21–26]. In the present study, an attempt was made to screen selected natural compounds for their TP inhibitory potential. Natural compounds present a long-standing tradition as valuable starting points in drug discovery program. Structural diversity makes them privileged sources for chemical probes. Medicinal plants are rich source of producing natural products and many of these are used as active ingredient of modern medicine [27–28]. Only less than 10% of the natural flora is investigated so far, therefore, nature holds a great promise for discovery of leads against most common, and emerging diseases [29].

Based on reported medicinal importance particularly the anti-cancer activity, some natural compounds belonging to class coumarin, flavonoid, carboxylic acid, alkaloid, and lignan were selected randomly and evaluated for their TP inhibitory activity [30–37]. These natural compounds are not reported earlier for the TP inhibitory activity. Isolation and spectroscopic data for the compounds are presented in the S1 Table. The current study led to the identification of new potential TP inhibitors, as summarized in Figs 1–4.

Materials and methods
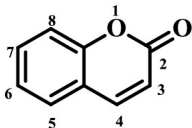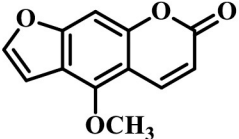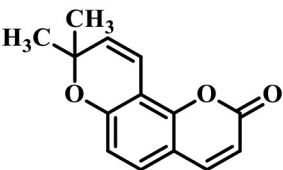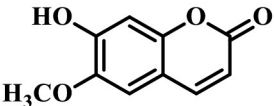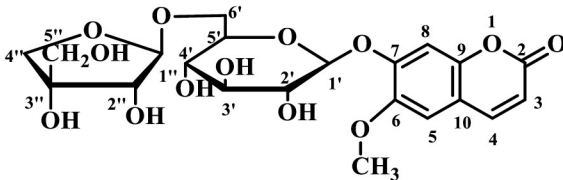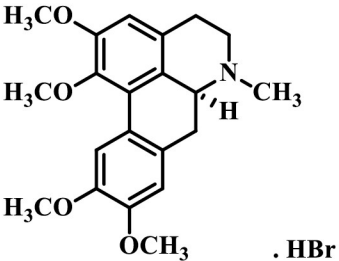
Enzyme thymidine phosphorylase (*E. coli*, E.C. No. 2.4.2.4, CAS # 9030-23-3), DMEM (Dulbecco's modified eagle medium, CAT # SLM-241), and cycloheximide (CAS # 66-81-9) were obtained from Sigma Aldrich, USA. DMSO (Dimethylsulfoxide, CAS # 67-68-5), and standard compounds (tipiracil; CAS # 183204-72-0, 7-deazaxanthine; CAS # 39929-79-8) were obtained from Fisher Scientific, Germany, and Santa Cruz Biotechnology Inc. (USA), respectively.

Compound	Structure	Plant Source	TP Inhibition IC$_{50}$ (μM ± SEM)*	Cytotoxicity IC$_{50}$ (μM± SD)§
	Flavonoids			
1		*Potentilla evestita* L.	**195.1 ± 1.1**	**29.05 ± 0.61**
2		*Eremostachys loasifolia* Benth.	**113.1 ± 0.9**	ND**
3		*Potentilla evestita* L.	**Inactive**	
4		*Potentilla evestita* L.	**Inactive**	
5		*Tegetes erecta* Linn.	**76.8 ± 1.8**	ND**

*IC$_{50}$ values are presented as mean ± standard error of mean; §IC$_{50}$ values are presented as mean ± standard deviation, ND** = Not determined because of low quantity, NC*** = Noncytotoxic,

Fig 1. Thymidine Phosphorylase Inhibitory Activity of Compounds 1–18.
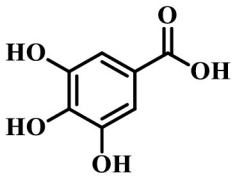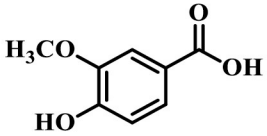
Compound	Structure	Plant Source	TP Inhibition IC$_{50}$ (μM $\pm$ SEM)*	Cytotoxicity IC$_{50}$ (μM$\pm$ SD)§
		Coumarins		
6		*Eremostachys vicaryi* Benth.	**420.3±6.15**	NC***
7		*Seseli diffusum* (Roxb. ex Sm.) Sant. & Wagh	**344.2 ± 1.2**	NC
8		*Seseli diffusum* (Roxb. ex Sm.) Sant. & Wagh	**181.1 ± 0.6**	NC
9		*Pauridiantha callicarpoides* (Hiern) Bremek.	**193.4 ± 1.0**	NC
10		*Pauridiantha callicarpoides* (Hiern) Bremek.	**295.2 ± 2.0**	NC
		Alkaloids		
11		*Glaucium flavum* Cr.	**238.5 ± 2.1**	NC

*IC$_{50}$ values are presented as mean ± standard error of mean; §IC$_{50}$ values are presented as mean ± standard deviation, ND** = Not determined because of low quantity, NC*** = Noncytotoxic,

Fig 2. Thymidine Phosphorylase Inhibitory Activity of Compounds 1–18 (Continued).
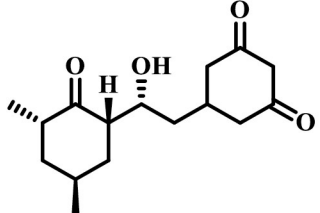
Compound	Structure	Plant Source	TP Inhibition IC$_{50}$ (μM ± SEM)*	Cytotoxicity IC$_{50}$ (μM± SD)§
12		*Berberis jaeschkeana* Schneid var. *jaeschkeana*	**Inactive**	
13		*Loranthus micranthus* Linn.	**Inactive**	
14		*Delphinium nordhagenii* Wendelbo	**Inactive**	
Carboxylic Acids				
15		*Spiraea brahuica* Boiss	**349.7 ± 1.4**	NC
16		*Ipomoea carnea* Jacq. ssp. fistulosa	**Inactive**	
17		*Bistorta manshuriensis* Komarov	**Inactive**	

*IC$_{50}$ values are presented as mean ± standard error of mean; §IC$_{50}$ values are presented as mean ± standard deviation, ND** = Not determined because of low quantity, NC*** = Noncytotoxic,

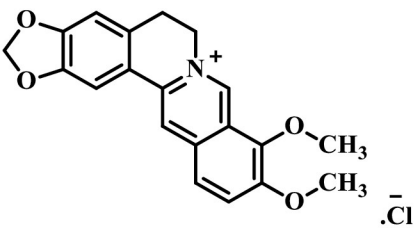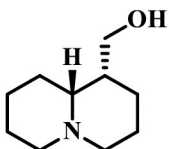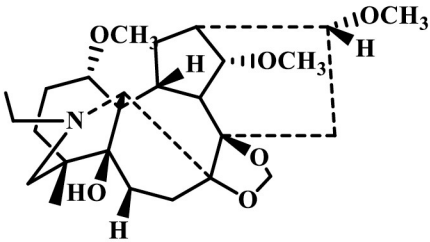**Fig 3. Thymidine Phosphorylase Inhibitory Activity of Compounds 1–18 (Continued).**

https://doi.org/10.1371/journal.pone.0225056.g003

Compound	Structure	Plant Source	TP Inhibition IC$_{50}$ (μM ± SEM)*	Cytotoxicity IC$_{50}$ (μM± SD)§
Lignan				
18		*Larrea nitida Cav.*	44.0 ± 0.5	NC
Standard (7-Deazaxanthine)$^\delta$			41.0 ± 1.63	--
Standard (Tipiracil)$^{\delta\delta}$			0.014 ± 0.002	--
Standard (Cyclohexamide)$^{\delta\delta\delta}$			-----	0.26 ± 0.1

*IC$_{50}$ values are presented as mean ± standard error of mean; §IC$_{50}$ values are presented as mean ± standard deviation, ND** = Not determined because of low quantity, NC*** = Noncytotoxic, $^\delta$, $^{\delta\delta}$, and $^{\delta\delta\delta}$ represents standard compounds used in the present study.

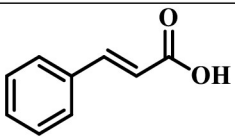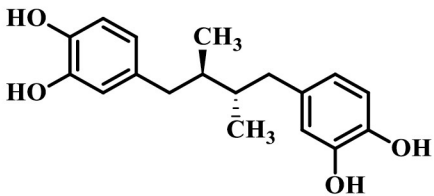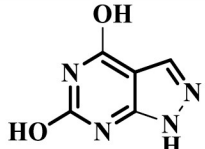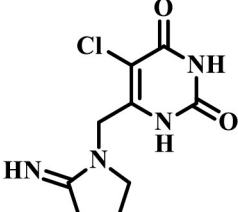**Fig 4. Thymidine Phosphorylase Inhibitory Activity of Compounds 1–18 (Continued).**

https://doi.org/10.1371/journal.pone.0225056.g004

K$_2$HPO$_4$ (Dipotassium hydrogen phosphate; CAS # 7758-11-4), and KH$_2$PO$_4$ (Potassium dihydrogen phosphate; CAS # 7778-77-0) were obtained from Merck, Germany. Mouse fibroblast cell line (3T-3, CAT # ATCC® CRL-1658™), 0.25% Trypsin EDTA (CAS # 25200056), FBS (fetal bovine serum; CAT # FBS-ES-22A), MTT (3-(4,5-dimethythiazol-2-yl)-2,5-diphenyl tetrazolium bromide, CAS # 298-93-1), and 0.4% Trypan Blue solution (CAS # K940) were obtained from American Type Culture Collection, USA, Gibco, Invitrogen, New Zealand, A&E Scientific, USA, MP Biomedicals, France, and Amersco, USA, respectively.

Source of natural compounds

Flavonoids. Compound **1** (CAS No. 525-82-6; purity ≥ 99% as indicated by HPLC), originally isolated from *Potentilla evestita* L., was purchased from Sigma Aldrich, USA. Compounds **2**, **3**, **4**, and **5** were isolated from *Eremostachys loasifolia* Benth., *Potentilla evestita* L., and *Tagetes patula* Linn., respectively [38–40]. These compounds **2–4** were > 99% pure as

assayed by HPLC techniques (See S1 Information and S1 Table for details about extraction and spectroscopic data).

Coumarins. Compound **6** was isolated from *Eremostachys vicaryi* Benth. Compounds **7–8** were isolated from *Seseli diffusum* (Roxb. ex Sm.) Sant. & Wagh, while **9–10** were isolated from *Pauridiantha callicarpoides* (Hiern) Bremek. These compounds were > 99% pure as assayed by HPLC techniques [41–43] (See S1 Information and S1 Table for details about extraction and spectroscopic data).

Alkaloids. Compounds **11** (Glaucine HBr, LOT No. 00007241–807; purity ≥ 94.9% from HPLC) and **12** (Berberine chloride, CAS No. 633-65-8; purity > 98% from TLC) isolated from *Glaucium flavum* Cranz. and *Berberis jaeschkeana* Schneid var. *jaeschkeana* respectively, were obtained from ChromaDex (Irvine, California, USA). Compound **13** (Lupinine, CAS No. 486-70-4; purity ≥ 97% from HPLC), isolated from *Loranthus micranthus* Linn. was bought from Santa Cruze Biotechnolgy Inc., USA, for the present study. Compound **14** (Nordhagenine A) was isolated from *Delphinium nordhagenii* Wendelbo [44] (See S1 Information and S1 Table for details about extraction and spectroscopic data).

Carboxylic acids. Compounds **15** (Cinnamic acid, CAS No. 140-10-3; purity ≥ 97% by titration with NaOH), **16** (Gallic acid, CAS No. 149-91-7; purity ≥ 97% by titration with NaOH), and **17** (Vanillic acid, CAS No. 121-34-6; purity ≥ 97% by titration with NaOH), originally isolated from *Spiraea brahuica* Boiss, *Ipomoea carnea* Jacq. ssp. fistulosa, and *Bistorta manshuriensis* Komarov. respectively, were purchased from Sigma Aldrich, USA (See S1 Information and S1 Table for details about extraction and spectroscopic data).

Lignan. Compound **18** (Masoprocol, CAS Number 500-38-9; purity ≥ 90% purity as assayed by HPLC) was purchased from Sigma Aldrich, USA. It was originally isolated from *Larrea nitida* Cav., (See S1 Information and S1 Table for details about extraction and spectroscopic data).

Thymidine phosphorylase inhibition assay. In the current study, we have used commercially available recombinant *E. coli* TP enzyme, as human TP is not easily accessible. Substantial similarities in terms of structural and active site residues exist between *E. coli* and mammalian TP enzymes, therefore *E. coli* TP generally serves as a primary model for the identification of lead inhibitors of TP [3].

Thymidine phosphorylase inhibition assay was carried out spectrophotometrically [45]. Briefly, 0.058 U of TP enzyme (E.C. No. 2.4.2.4, *E. coli*) was incubated with 500 μM of test compounds at 30°C for 10 minutes. After that 1.5 mM of substrate thymidine was added to 96-well plate, and changes in absorbance were monitored for 10 minutes at 290 nm in microtiter plate reader (Spectramax, M5, Molecular Devices, CA, USA). Enzyme and substrate solution were prepared in 50 mM phosphate buffer of pH 7.0, while test compounds were prepared in DMSO (final concentration 4.5%). Tipiracil and 7-deazaxanthine were used as standard inhibitors, and each experiment was performed in triplicate.

Mechanistic studies. In mechanistic studies, TP enzyme was incubated with different concentrations of inhibitors at 30°C for 10 min. Reaction was then initiated by adding four different concentrations of substrate, *i.e.* thymidine (0.1875–1.5 mM). Enzyme activity was measured under steady state conditions by measuring changes in absorbance for another 10 min at 30°C at 290 nm, on microtiter plate reader (Spectramax, M5, Molecular Devices, CA, USA). Every experiment is performed in triplicate.

Molecular docking studies

Ligand preparation. Prior to docking, the molecules (ligands) were processed *via Ligprep* module in Maestro Schrödinger 10.5. It involves the generation of low energy 3-D structures

from 2-D structures of compounds in SD format. Possible ionization states and correct protonation were generated using *Epik* module which predict the tautomeric state, and generate energetic penalties for each molecule conformation it predicts [46].

Protein preparation. X-Ray crystallographic structure of *E. coli* TP was used for docking studies (PDB ID: 4LHM). Maestro Schrödinger software was used to prepared protein by employing the *Protein Preparation Wizard* 10.5 [47, 48]. OPLS-2005 force field was used to add missing hydrogens, and for the assignment of partial charges. Optimization of heavy atoms and hydrogens was then carried out by subjecting the structure to restrained minimization. The co-crystallized water molecules were retained because they were present in the active site, involving the formation of general hydrogen bond network. Since the sulfate ion was replaced with phosphate, it occupied the same place in active site in crystal structure as that of phosphate ion.

Searching for allosteric binding sites and molecular docking analysis. To find out the allosteric site for non-competitive and uncompetitive inhibitors, site recognition software Site-Map 3.7 [49, 50] Maestro version 10.5 from Schrödinger was run on crystal structure to identify the top 5 ranked potential ligand-binding pockets.

The grid box with dimensions of 15Å x 15Å x 15Å was defined to confine the mass of centre of each docked ligand. Extra precision (XP) mode of Glide based on OPLS-2005 force field was run for rigid receptor docking protocol [51–54]. Molecular mechanics-generalized Born surface area (MM-GBSA) method in Prime was used for rescoring the docked pose of ligand [55]. These poses were taken as inputs for the energy minimization of the protein–ligand complexes ($E_{complex}$), the free protein ($E_{receptor}$), and the free ligands (E_{ligand}). The binding free energy ΔG_{bind} was determined according to the following equation:

$$\Delta G_{bind} = E_{complex\ (minimized)} - E_{ligand\ (minimized)} - E_{receptor\ (minimized)}$$

In vitro cytotoxicity assay

Cytotoxicity of active compounds was evaluated spectrophotometrically by standard MTT (3-[4,5-dimethylthiazole-2-yl]-2,5-diphenyl-tetrazolium bromide) assay, following the method of Demas *et al*. In cytotoxicity assay, reduction of MTT dye to formazan by mitochondrial enzyme (succcinate dehydogenase) is measured. The reduction of MTT can only occur in metabolically active cell, so the enzyme activity is actually a measure of cell viability [24, 56].

Briefly, the mouse fibroblast cells (3T3) were cultured in DMEM media containing 5% FBS, 100 IU/ mL penicillin, and 100 μg/ mL streptomycin. Cell suspension (5×10^4cells/ mL) was dispensed in flat-bottomed 96-well plates, and incubated at 37˚C and with 5% CO_2. After the overnight incubation, old media was aspirated and fresh media containing different concentrations of compounds (prepared in DMSO) were added, and plate was further incubated for 48 hrs. After that, MTT dye (0.5 mg/ mL) was added into each well, and the plate was further incubated for 4 hrs. Following this, DMSO (100 μL) was added into each well, and the level of MTT reduction to formazan with in the cells was calculated by taking the absorbance at 540 nm using a micro plate reader (Spectra Max plus, Molecular Devices, CA, USA).

Analysis of the experiments

In vitro **TP spectrophotometric assay.** Enzyme activity was measured under steady-state conditions by observing changes in absorbance for 10 min (at 290 nm) on microtiter plate reader (Spectra Max M5, Molecular Devices, CA, USA). Changes in absorbance upon addition of test compounds were analyzed with the SoftMax Pro 4.8 software which was purchased from Molecular Devices, CA, USA. To calculate the percent inhibition, following formula was

used:

$$\% \, Inhibition \, = \, 100 - \frac{Absorbance \, of \, test \, compound}{Absorbance \, of \, control} \times 100$$

Inhibitory potential of test compounds is represented in Figs 1–4 as IC_{50} value (Inhibitory concentration). The IC_{50} represents concentration of compounds that inhibit the degradation of thymidine to thymine by 50%. It was calculated by measuring the effects of different concentrations of inhibitors on the degradation of thymidine. EZ-Fit, Enzyme kinetics software (purchased from Perrella Scientific, Inc., USA) was used to deduce the IC_{50} values.

Analysis of mechanistic assay

Mechanistic studies were performed to find out the mechanism of inhibition of active compounds. Lineweaver-Burk plot was used to determine the type of inhibition, where the reciprocal of rate of the reaction were plotted against the reciprocal of substrate concentration. Dissociation constant (K_i) were determined by secondary re-plot of Lineweaver-Burk plots. Kinetic data was analysed by GraFit 7 data analysis software (purchased from Erithacus Software Limited, UK) [57].

Analysis of docking studies

To find out the allosteric site for non-competitive and uncompetitive inhibitors, site recognition software SiteMap 3.7 Maestro version 10.5 from Schrödinger was run on crystal structure to identify the top 5 ranked potential ligand-binding pockets. Molecular mechanics-generalized Born surface area (MM-GBSA) method in Prime was used for rescoring the docked pose of ligand. The binding free energy ΔG_{bind} was determined according to the–equation given earlier.

Analysis of cytotoxicity assay

The cytotoxicity was recorded as concentration causing 50% growth inhibition (IC_{50}) for 3T3 cells. Cellular viability was measured for 10 min, at 570 nm on microtiter plate reader. Changes in absorbance upon addition of test compounds were analyzed with the SoftMax Pro 4.8 software which was purchased from Molecular Devices, CA, USA. Percent inhibition was calculated using the formula mentioned earlier.

Cytotoxicity potential of test compounds is represented in Figs 1–4 as IC_{50} values. The IC_{50} represents concentration of compounds that inhibit the cell growth by 50%. It was calculated by measuring the effects of different concentrations of inhibitors on the growth of cells. EZ-Fit, Enzyme kinetics software was used to deduce the IC_{50} values.

Results and discussion

Eighteen secondary metabolites of medicinal plant origin were evaluated for their *in vitro* TP inhibitory activity *via* biochemical method. Eleven compounds **1**, **2**, **5–10**, **11**, **15**, and **18** exhibited good to weak TP inhibitory activity with IC_{50} values between 44.0 to 420.3 μM, as compared to the standard inhibitor, 7-deazaxanthine (7-DX) (IC_{50} = 41.0 ± 1.63 μM). The results indicate that these compounds are effective at high micromolar concentration thus could serve as starting point for the development of new anti-TP molecules. Limited structure-activity relationship was carried out (explained below) as the current study is based on the small number of compounds.

Structure-activity relationship of natural compounds

Among compounds **1–5** belonging to flavonoid class, **1**, **2**, and **5** showed a good to weak TP inhibiting ability with IC_{50} values of 76.8 to 195.1 μM, as compared to standard 7-deazaxanthine ($IC_{50} = 41.0 \pm 1.63$ μM), while compounds **3**, and **4** were found to be inactive.

Compound **1** with a basic flavonoid skeleton showed a weak TP inhibiting activity ($IC_{50} = 195.1 \pm 1.1$ μM). Compound **2** with OH groups at C-5, C-2', and C-3', and OCH_3 groups at C-7 and C-6' showed a good TP inhibition ($IC_{50} = 113.0 \pm 0.9$ μM), as compared to compound **1**. However, presence of OH groups at C-5, C-7 and C-4', as in compound **3**, and at C-5 and C-7, as in compound **4** were found unfavourable for TP inhibition. Presence of OCH_3 at C-6 and OH at C-3, C-5, C-7, C-4', and C-5' in compound **5** enhanced the TP inhibitory potential ($IC_{50} = 76.8 \pm 1.1$ μM). Structure-activity relationship (SAR) indicated that number and position of electron donating groups on flavonoid nucleus play role in TP inhibition. Hydroxyl and methoxy groups are expected to form hydrogen bonds and/or hydrophobic interactions with amino acid residues at active site or hydrophobic pocket of the TP enzyme.

Compounds **6–10** of coumarins class showed a weak TP inhibiting activity with IC_{50} values in the range of 181.1–420.3 μM, as compared to the standard 7-deazaxanthine ($IC_{50} = 41.0 \pm 1.63$ μM) (Table 1). Among the group, compound **6** showed the weakest TP inhibition ($IC_{50} = 420.3 \pm 6.15$ μM). Presence of furan and methoxy moieties at coumarin skeleton in compound **7** increased the inhibitory potency ($IC_{50} = 344.2 \pm 1.2$ μM), as compared to compound **6**. TP inhibition increased further due to the presence of pyran and di-methyl groups at coumarin skeleton, as in compound **8** ($IC_{50} = 181.1 \pm 0.6$ μM). Compound **9** with OH and OCH_3 groups on coumarin skeleton also showed the increased TP inhibitory potential in comparison to compound **6** ($IC_{50} = 193.4 \pm 1.0$ μM). However, replacement of hydroxyl group at C-7 with apiose glucoside moiety in compound **10** decreased the TP inhibition potency ($IC_{50} = 295.2 \pm 2.0$ μM). This indicates that OH group is critical for inducing enzyme inhibition.

SAR suggested that compound **6** (coumarin) is mainly interacting with the enzyme *via* hydrophobic interaction with critical residues at the active site or hydrophobic pocket of enzyme TP. The presence of other electron donating groups (hydroxyl and methoxy) in compounds **7–10**, found to enhance their potential of inhibiting the TP enzyme, in comparison to compound **6**. Hydroxyl may likely to be involve in forming hydrogen bond with the amino acids at active site or hydrophobic pocket of the TP enzyme.

Among the alkaloids **11–14**, compound **11** exhibited a weak TP inhibitory activity ($IC_{50} = 238.5 \pm 2.1$ μM). Methoxy groups of compound **11** proposed to interact with the enzyme's hydrophobic pocket *via* hydrogen bonding with critical amino acid residues. Compounds **12–14** were found to be inactive against the TP.

Table 1. Kinetic data of compounds 1, 5–11, and 18.

Compound	$Ki \pm SEM^a$ (μM)	Type of inhibition
1	225.0 ± 0.002	Uncompetitive
5	341.1 ± 0.01	Mixed
6	171.0 ± 0.001	Uncompetitive
8	162.0 ± 0.001	Uncompetitive
9	419.0 ± 0.001	Non-competitive
10	145.0 ± 0.001	Uncompetitive
11	180.0 ± 0.01	Uncompetitive
18	25.6 ± 0.008	Competitive
7-Deazaxanthine	45.66 ± 0.0009	Non-competitive

[a]$Ki \pm SEM$ is dissociation constant ± Standard Error of the Mean

Among the compounds **15–17** belonging to benzoic acid class, only compound **15** showed a weak TP inhibitory activity with IC_{50} of 349.7 ± 1.4 μM. This compound is likely to be engaged in hydrogen bonding with the residues present at the active site or hydrophobic pocket of the enzyme. However, the phenyl moiety can also be involved in π-π interaction with aromatic residues. Compounds **16**, and **17** were found to be inactive.

Compound **18**, a lignan, exhibited a significant TP inhibitory activity (IC_{50} = 44.0 ± 0.5 μM). Hydroxyl groups are apparently forming hydrogen bonds with critical amino acid residues of the active site.

Mechanistic studies

Mechanistic studies were performed on the selected natural products. It was found that they inhibit TP enzyme in a concentration-dependent manner with dissociation constant (*K*i) values between 25.6–419.0 μM. Natural products **5**, **9**, and **18** exhibited mixed, non-competitive, and competitive modes of inhibition, respectively, while natural compounds **1**, **6**, **8**, **10**, and **11** showed an uncompetitive type of inhibition (Table 1, Figs 5–8). Lineweaver-Burk plot was plotted to determine the inhibition type, secondary re-plot of Lineweaver-Burk plot was used to deduce (*K*i) values.

Molecular docking studies

Sitemap analysis was run for non-competitive, uncompetitive, and mixed inhibitors to identify the potential allosteric binding site of the enzyme. Among the 5 top ranked sites, the druggable site with highest site score of 1.05 was chosen as allosteric site with respect to the thymidine for docking studies.

The docking analysis revealed that all of the *in silico* predicted lowest energy complexes were stabilized by stacking interaction, and intermolecular hydrogen bonds. Compound **1** having the primary flavonoid scaffold, form hydrogen bonds with Arg 171, while compound **5** with OH and OCH_3 substitutions form π-cation interaction with Arg 171. π-π interactions were also observed with Phe 210 (Fig 9A and 9B).

A   B

Fig 5. The inhibition of TP by compound 5, (A) is the Lineweaver-Burk plot of reciprocal rate of reaction (velocities) *verses* reciprocal of substrate (thymidine) in the absence (▼), and in the presence of 230 μM (○), 110 μM (Δ), 80 μM (▲) and 50 μM (▽) of compound **5**. (B) is secondary replot of Lineweaver-Burk plot between the slopes of each line on Lineweaver-Burk plot *versus* different concentrations of compound **5**.
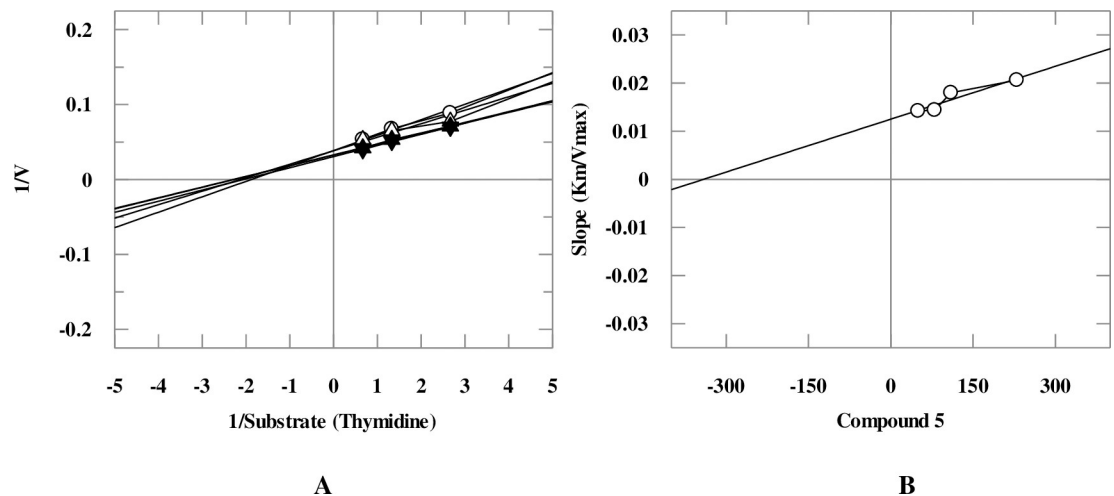
Fig 6. The inhibition of TP by compound 9, (A) is the Lineweaver-Burk plot of reciprocal rate of reaction (velocities) *verses* reciprocal of substrate (thymidine) in the absence (▼), and in the presence of 300 μM (○), 200 μM (Δ), 100 μM (▲) and 50 μM (▽) of compound **9**. (B) is secondary replot of Lineweaver-Burk plot between the slopes of each line on Lineweaver-Burk plot *versus* different concentrations of compound **9**.
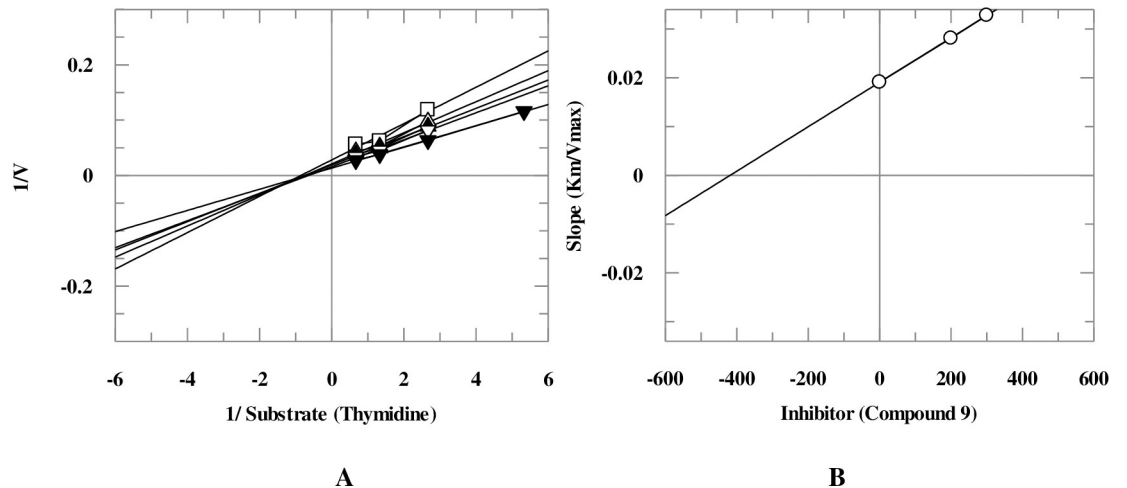
MMGBSA score provides the predictive binding affinity of the ligand binding to the protein. A more negative score is indicative of better binding affinity towards corresponding ligand molecule. Analysis of MMGBSA score revealed that compounds **1**, and **5** have predictive binding energies of -40.45, and -61.99 kcal/mol, respectively, which is in agreement with their experimental Ki values *i.e.*, 225 and 150 μM, respectively.

Molecular docking of coumarins with TP showed that compound **6** form only π-π interaction through its pyran ring with Phe210 (Fig 10A). The dimethyl pyran ring in compound **8** made π-cation interaction with Arg171 (Fig 10B). Presence of hydroxyl and methoxy groups in compound **9** form hydrogen bonds with Arg171, and Ser186, along with π-π interaction with Phe 210 (Fig 10C). Compound **10** showed π-cation interaction *via* its benzyl moiety to

Fig 7. The inhibition of TP by compound 11, (A) is the Lineweaver-Burk plot of reciprocal rate of reaction (velocities) *verses* reciprocal of substrate (thymidine) in the absence (▼), and in the presence of 300 μM (■), 250 μM (Δ), and 200 μM (▲) compound **11**. (B) is secondary replot of Lineweaver-Burk plot between the slopes of each line on Lineweaver-Burk plot *versus* different concentrations of compound **11**.
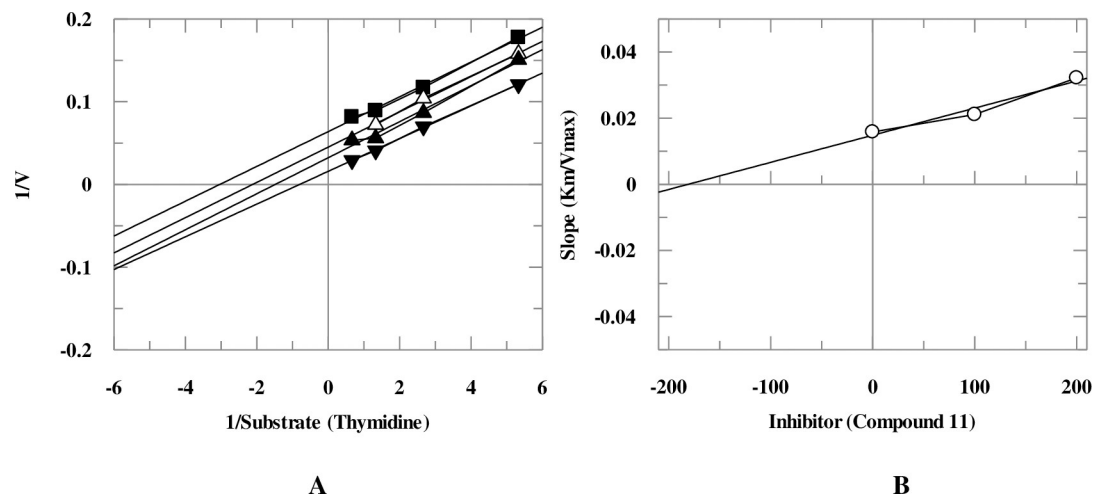
Fig 8. The inhibition of TP by compound 18, (A) is the Lineweaver-Burk plot of reciprocal rate of reaction (velocities) *verses* reciprocal of substrate (thymidine) in the absence (▾), and in the presence of 80 μM (□), 60 μM (■), and 50 μM (Δ) of compound **18**. (B) is secondary replot of Lineweaver-Burk plot between the slopes of each line on Lineweaver-Burk plot *versus* different concentrations of compound **18**.
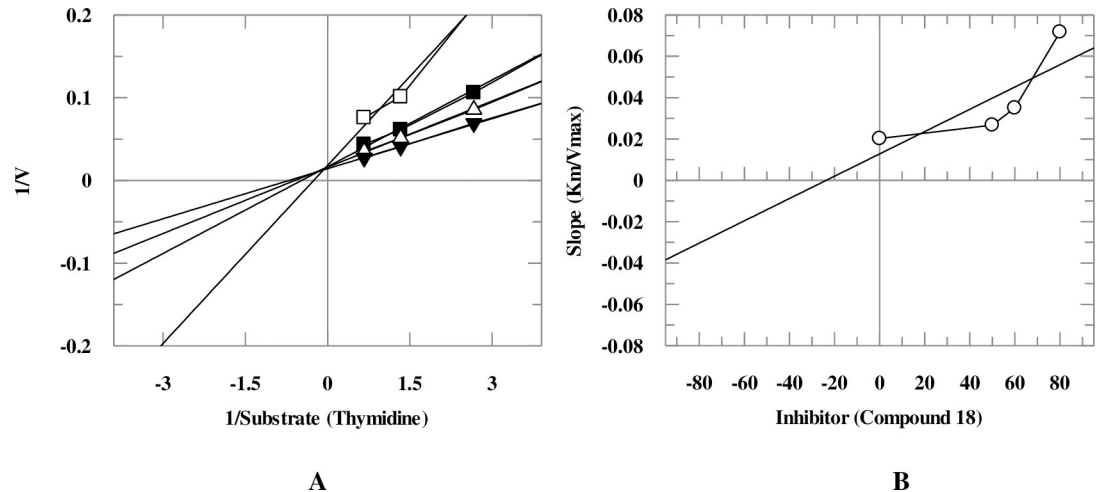
Arg171, while the furan ring made hydrogen bonds with Gly121, and Thr123 ([Fig 10D]). Correlation between the experimental *K*i values and predictive binding affinities (*via* MMGBSA scoring) were also observed in coumarins **6, 8**, and **10**. Compound **10** with *K*i value 145.0 ± 0.001 μM has exhibited the highest binding affinity with MMGBSA score of -91.01 kcal/mol. This can be attributed to the large size of the molecule that helped it to better accommodate into the allosteric site. Compounds **6** (*K*i = 171 ± 0.001 μM), and **8** (*K*i = 162.0 ± 0.001 μM) showed the predictive binding energies of -39.85, and -54.53 kcal/mol, respectively. Despite being substituted derivative of compound **6**, compound **9** did not show any correlation between experimental *K*i value and MMGBSA score relative to other derivatives of compound **6** *i.e.*, compounds **8,** and **10**. The MMGBSA score for compound **6** was found to be -44.90 kcal/mol with *K*i value of 419.0 ± 0.001 μM.

Fig 9. 3D modelled pose of (a) compound 1, and (b) compound 5 *via* docking in the sitemap predicted binding site of *E. coli* TP. Hydrogen bonds are represented as black dotted lines. π-π and π-cation interactions are represented as blue and green dotted lines, respectively.

a

b

c

d

Fig 10. 3D modelled pose of (a) compound 6 (b) compound 8 (c) compound 9 and (d) compound 10 *via* docking in the sitemap predicted binding site of *E. coli* TP. Hydrogen bonds are represented as black dotted lines. π-π and π-cation interactions are represented as blue and green dotted lines, respectively.
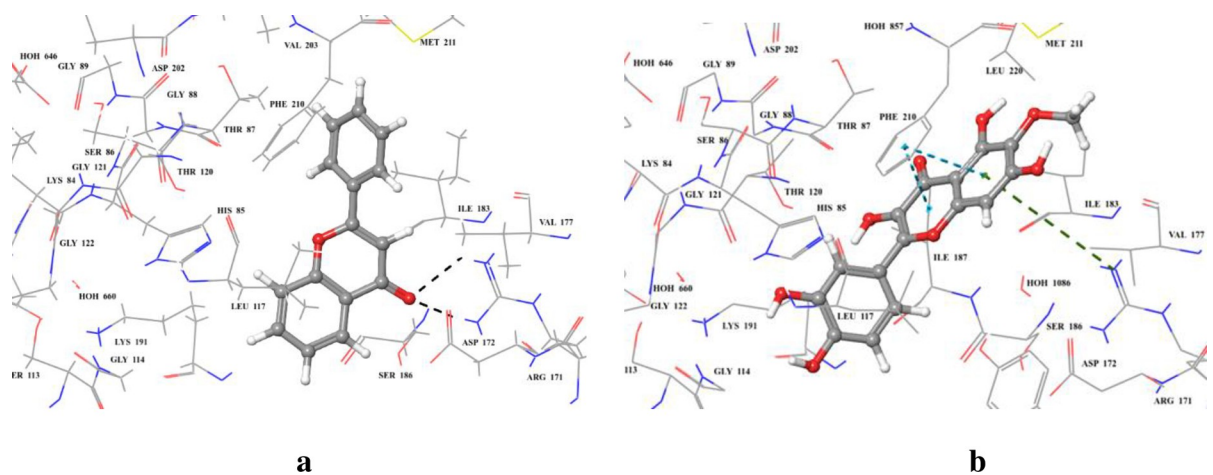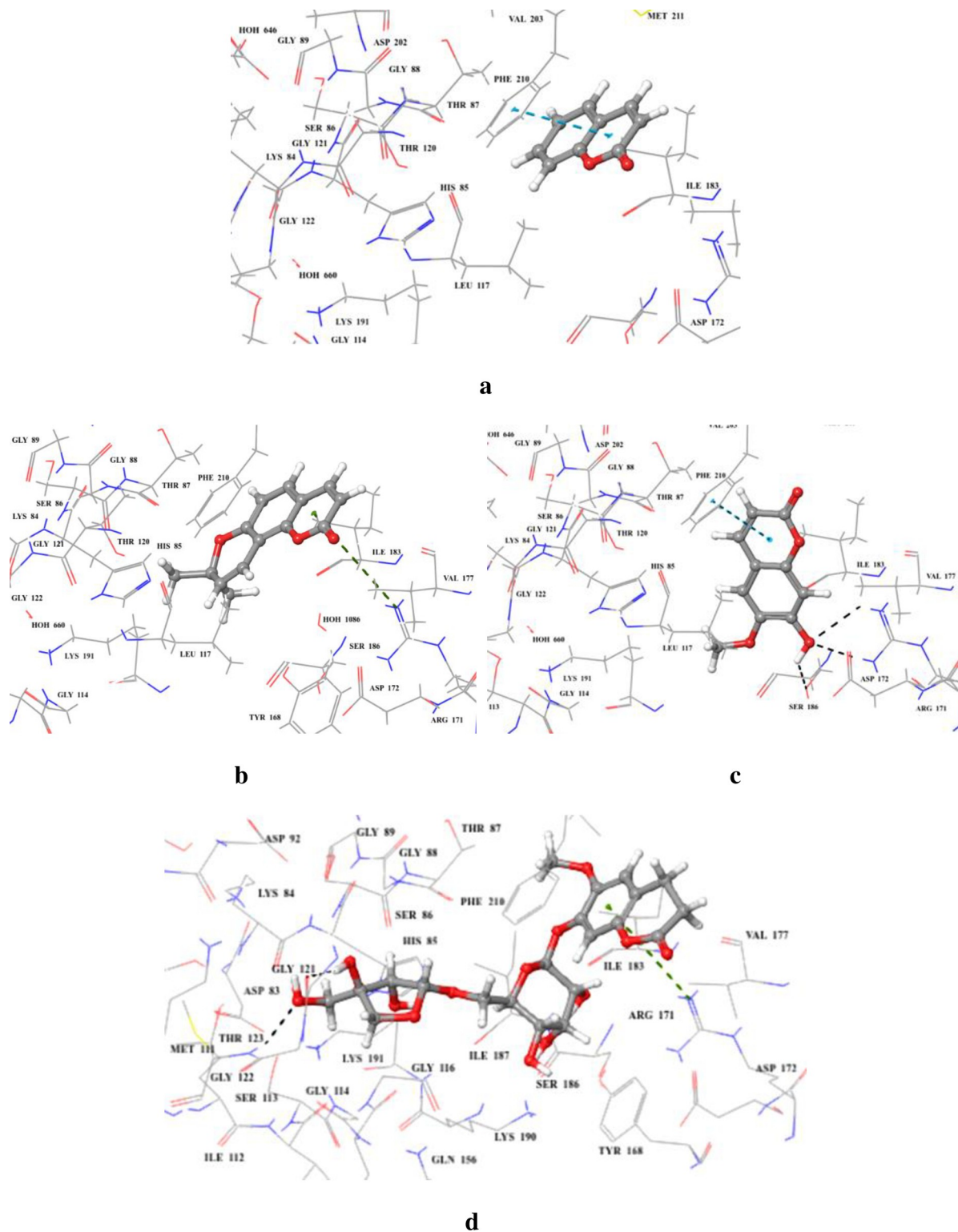
https://doi.org/10.1371/journal.pone.0225056.g010
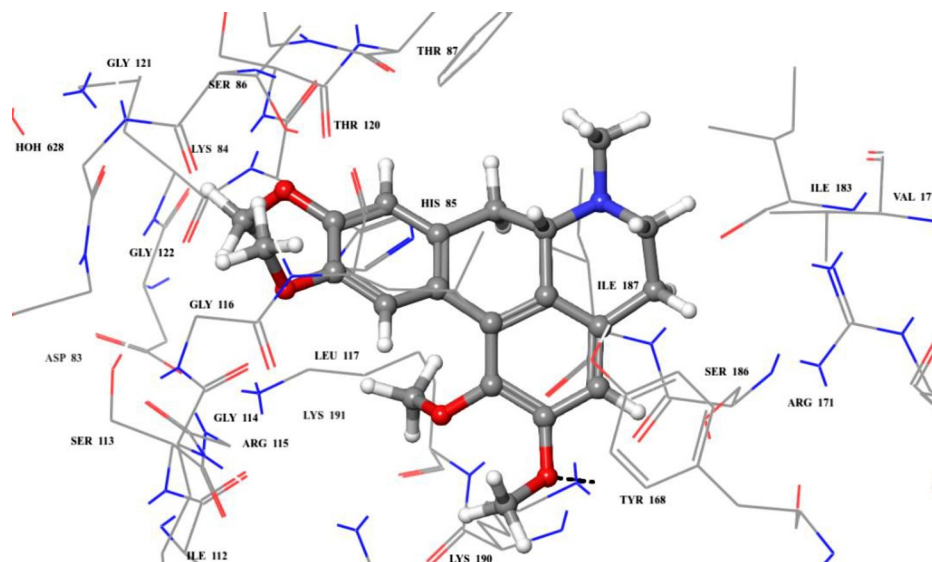
Fig 11. 3D modelled pose of (a) compound 11 *via* docking in the sitemap predicted binding site of *E. coli* TP. Hydrogen bonds are represented as black dotted lines.

Molecular docking studies also showed that compound **11** had only one hydrogen bond with Lys 190 *via* one of its dimethoxy benzyl moieties ([Fig 11]). The predictive binding energy (ΔG_{bind}) was found to be -41.79 kcal/mol.

Compound **18** of carboxylic acid class was found to be competing with thymidine for binding (competitive inhibitor); therefore it was docked into the substrate binding site of TP. Analysis of docking result showed that compound **18** adopted a different binding pose than substrate thymidine. One of the dihydroxy benzyl moieties interacted *via* π-cation interaction to Tyr 168. While the attached OH groups form hydrogen bonds with Arg 171, and Ile 183. The other dihyroxy benzyl group form hydrogen bonds with phosphate ion in substrate binding site ([Fig 12]). The compound was rescored *via* MMGBSA, and turned out to give predictive binding energy of about -60 kcal/mol.

Cytotoxicity assay

Compounds **1**, **6–11**, **15**, and **18** were finally subjected to cytotoxicity MTT assay on 3T3 cell line. Compound **1** showed a weak growth inhibition of 3T3 cells (IC_{50} = 29.05 ± 0.61μM) in comparison to standard cycloheximide (IC_{50} = 0.20 ± 0.10 μM), while compounds **6–11**, **15**, and **18** were found to be non-cytotoxic. These compounds are, therefore, promising leads to be investigated further for *in vivo* anti- cancer and other relevant therapeutic activities.

Conclusions

Many solid tumors have over-expression of thymidine phosphorylase (TP). TP assists cancer progression by inducing angiogenesis and preventing apoptosis. These critical functions make it an ideal target for the development of anti-angiogenic compounds. This systematic study identifies several natural products as anti-TP molecules with inhibitory activity good to weak, in comparison to the standard 7-deazaxanthine. Masoprocol (**18**), a dicatechol isolated from the *Larrea divaricata* Cav., showed the significant TP inhibitory activity, among all the natural products evaluated. It was found to interact with the active site residues of TP in kinetic studies (competitive inhibitor); however it exhibited a different binding pose than the natural

Fig 12. 3D modelled pose of compound 18 *via* docking in the active site (thymidine binding site) of *E. coli* TP. Hydrogen bonds are represented as black dotted lines. π-π and π-cation interactions are represented as blue and green dotted lines, respectively.
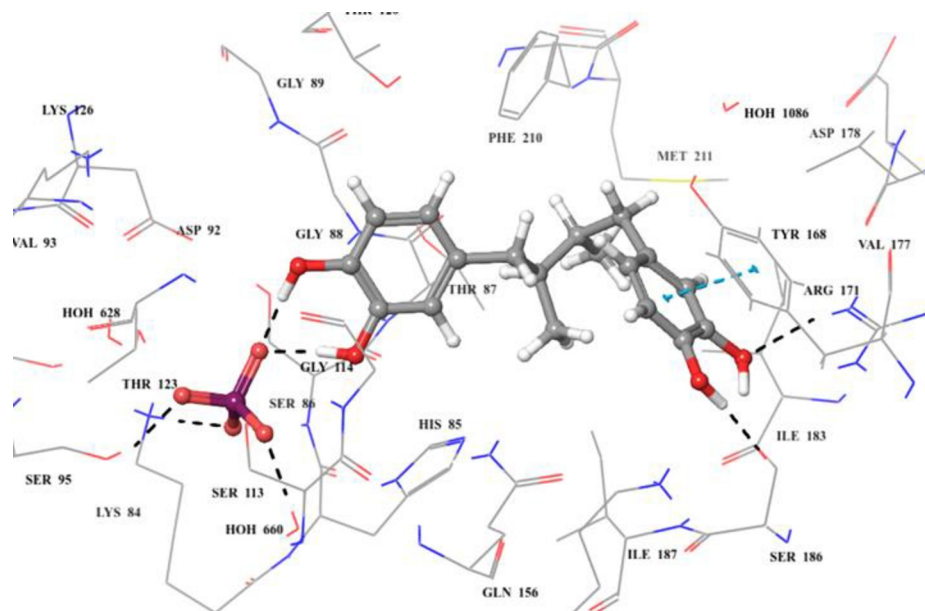
https://doi.org/10.1371/journal.pone.0225056.g012

substrate in *in silico* studies. Furthermore, it was non-cytotoxic to mouse fibroblast cells (3T3). These compounds can serve as leads for the development of new anti-angiogenic molecules.

Supporting information

S1 Information. Plant material used, extraction and isolation of natural compounds. (DOCX)

S1 Table. Isolation and spectroscopic data of the natural compounds 1–18. (DOCX)

Acknowledgments

Author Contributions

Conceptualization: M. Iqbal Choudhary.

Data curation: Muniza Shaikh, M. Iqbal Choudhary.

Formal analysis: Sumaira Javaid, M. Iqbal Choudhary.

Investigation: Sumaira Javaid, M. Iqbal Choudhary.

Methodology: Sumaira Javaid, Muniza Shaikh, Narjis Fatima, M. Iqbal Choudhary.

Project administration: M. Iqbal Choudhary.

Software: Sumaira Javaid, Muniza Shaikh, M. Iqbal Choudhary.

Supervision: M. Iqbal Choudhary.

Validation: M. Iqbal Choudhary.

Writing – original draft: Sumaira Javaid, Muniza Shaikh, M. Iqbal Choudhary.

Writing – review & editing: Sumaira Javaid, Muniza Shaikh, M. Iqbal Choudhary.

References

1. de Moura Sperotto ND, Deves Roth C, Rodrigues-Junior VS, Ev Neves C, Reisdorfer Paula F, da Silva Dadda et al., 2019. Design of novel inhibitors of human thymidine phosphorylase: Synthesis, enzyme inhibition, *in vitro* toxicity, and impact on human glioblastoma cancer. J Med Chem. 2019; 62:1231–1245. https://doi.org/10.1021/acs.jmedchem.8b01305 PMID: 30615449

2. Brown NS, Bicknell R. Thymidine phosphorylase, 2-deoxy-D-ribose and angiogenesis. Biochem J. 1998; 334: 1–8. https://doi.org/10.1042/bj3340001 PMID: 9693094

3. Bronckaers A, Gago F, Balzarini J, Liekens S. The dual role of thymidine phosphorylase in cancer development and chemotherapy. Med Res Rev. 2009; 29: 903–953. https://doi.org/10.1002/med.20159 PMID: 19434693

4. Fox SB, Westwood M, Moghaddam A, Comley M, Turley H, Whitehouse RM, et al., The angiogenic factor platelet-derived endothelial cell growth factor/thymidine phosphorylase is up-regulated in breast cancer epithelium and endothelium, Br J Cancer. 1996; 73: 275–280. https://doi.org/10.1038/bjc.1996.49 PMID: 8562330

5. Takebayashi Y, Akiyama S, Akiba S, Yamada K, Miyadera K, Sumizawa T, et al., Clinicopathologic and prognostic factor significance of an angiogenic factor thymidine phosphorylase in human colorectal carcinoma, J. Natl. Cancer Inst. 1996; 88:1110–1117. https://doi.org/10.1093/jnci/88.16.1110 PMID: 8757190

6. O' Brien TS, Fox SB, Dickinson AJ, Turley H, Westwood M, et al. Expression of the angiogenic factor thymidine phosphorylase/platelet-derived endothelial cell growth factor in primary bladder cancers. Cancer Res. 1996; 56: 4799–4804. PMID: 8841001

7. Igarashi M, Dhar DK, Kubota H, Yamamoto A, El-Assal O, Nagasue N. The prognostic significance of microvessel density and thymidine phosphorylase expression in squamous cell carcinoma of the esophagus. Cancer. 1998; 82:1225–1232. https://doi.org/10.1002/(sici)1097-0142(19980401)82:7<1225::aid-cncr3>3.0.co;2-e PMID: 9529012

8. de-Bruin M, Temmink OH, Hoekman K, Pinedo HM, Peters GJ. Role of platelet derived endothelial cell growth factor / thymidine phosphorylase in health and disease. Cancer Ther. 2006; 4:954–967.

9. Miyadera K, Emura T, Suzuki N, Akiyama S, Fukushima M, Yamada Y. Novel functional antitumor nucleoside TAS-102, combined form of F3dThd and its modulator (2): Inhibitory effect of TPI on tumor-derived angiogenesis and metastasis. Proc Natl Assoc Cancer Res. 1998; 39: 609.

10. Matsushita S, Nitanda T, Furukawa T, Sumizawa T, Tani A, Nishimoto K, et al. The effect of a thymidine phosphorylase inhibitor on angiogenesis and apoptosis in tumors. Cancer Res. 1999; 59:1911–1916. PMID: 10213500

11. Pomeisl K, Votruba I, Holy A, Pohl R. Syntheses of pyrimidine acyclic nucleoside phosphonates as potent inhibitors of thymidine phosphorylase (PD-ECGF) from SD-lymphoma. Nucleos Nucleot Nucl. 2007; 26:1025–1028.

12. Gbaj A, Edwards PN, Reigan P, Freeman S, Jaffar M, Douglas KT. Thymidine phosphorylase from *Escherichia coli*: Tight-binding inhibitors as enzyme active-site titrants. J Enzyme Inhib Med Chem. 2006; 21:69–73. https://doi.org/10.1080/14756360500424010 PMID: 16570508

13. Nencka R, Votruba I, Hrebabecky H, Jansa P, Tloustova E, Horska K, et al., Discovery of 5-substituted-6-chlorouracils as efficient inhibitors of human thymidine phosphorylase. J Med Chem. 2007; 50:6016–6023. https://doi.org/10.1021/jm070644i PMID: 17963370

14. McNally VA, Rajabi M, Gbaj A, Stratford IJ, Edwards PN, Douglas KT, et al., Design, synthesis and enzymatic evaluation of 6-bridged imidazolyluracil derivatives as inhibitors of human thymidine phosphorylase. J Pharm Pharmacol. 2007; 59:537–547. https://doi.org/10.1211/jpp.59.4.0008 PMID: 17430637

15. Liekens S, Balzarini J, Hernández AI, De Clercq E, Priego EM, Camarasa MJ, et al., Thymidine phosphorylase is noncompetitively inhibited by 5'-O-trityl-inosine (KIN59) and related compounds. Nucleos Nucleot Nucl. 2006; 25: 975–980.

16. Casanova E, Hernandez AI, Priego EM, Liekens S, Camarasa MJ, Balzarini J, et al.,5'-O-Tritylinosine and analogues as allosteric inhibitors of human thymidine phosphorylase. J Med Chem. 2006; 49:5562–5570. https://doi.org/10.1021/jm0605379 PMID: 16942029

17. Mayer RJ, Cutsem EV, Falcone A, Yoshino T, Garcia-Carbonero R, Mizunuma N, et al., Randomized trial of TAS-102 for refractory metastatic colorectal cancer. New Engl J Med. 2015; 372:1909–1919. https://doi.org/10.1056/NEJMoa1414325 PMID: 25970050

18. Balzarini J, Gamboa AE, Esnouf R, Liekens S, Neyts J, De Clercq E, et al., 7-Deazaxanthine, a novel prototype inhibitor of thymidine phosphorylase. FEBS Lett. 1998; 438:91–95 https://doi.org/10.1016/s0014-5793(98)01271-x PMID: 9821965

19. Liekens S, De Clercq E, Neyts J. Angiogenesis: Regulators and clinical applications. Biochem Pharmacol. 2001; 61: 253–270. https://doi.org/10.1016/s0006-2952(00)00529-3 PMID: 11172729

20. Liekens S, Bilsen F, De Clercq E, Priego EM, Camarasa MJ, Pérez-Pérez MJ, et al., Anti-angiogenic activity of a novel multi-substrate analogue inhibitor of thymidine phosphorylase. FEBS Lett. 2002; 510: 83–88. https://doi.org/10.1016/s0014-5793(01)03233-1 PMID: 11755536

21. Khan KM, Ambreen N, Hussain S, Perveen S, Choudhary MI. Schiff bases of 3-formylchromone as thymidine phosphorylase inhibitors. Bioorg Med Chem. 2009; 17:2983–2988. https://doi.org/10.1016/j.bmc.2009.03.020 PMID: 19329330

22. Khan KM, Rani M, Ambreen N, Ali M, Hussain S, Perveen S, et al., 2,5-Disubstituted-1,3,4-oxadiazoles: Thymidine phosphorylase inhibitors. Med Chem Res. 2013; 22: 6022–6028.

23. Javaid S, Saad SM, Perveen S, Khan KM, Choudhary MI. 2-Arylquinazolin-4(3H)-ones: A novel class of thymidine phosphorylase inhibitors. Bioorg Chem. 2015; 63:142–151. https://doi.org/10.1016/j.bioorg.2015.10.006 PMID: 26547232

24. Javaid S, Ishtiaq M, Shaikh M, Hameed A, Choudhary MI. Thymidine esters as substrate analogue inhibitors of angiogenic enzyme thymidine phosphorylase *in vitro*. Bioorg Chem. 2017; 70: 44–56. https://doi.org/10.1016/j.bioorg.2016.11.007 PMID: 27955923

25. Hussain S, Gaffney J, Ahmed N, Slevin M, Choudhary MI, Ahmad VU, et al., An investigation of the kinetic and anti-angiogenic properties of plant glycoside inhibitors of thymidine phosphorylase. J Asian Nat Prod Res. 2009; 11:159–167. https://doi.org/10.1080/10286020802618860 PMID: 19219729

26. Abbasi MA, Ahmad VU, Zubair M, Fatima N, Farooq U, Hussain S, et al., Phosphodiesterase and thymidine phosphorylase inhibiting Salirepin derivatives from *Symplocos racemosa*. Planta Med. 2004; 70:1189–1194. https://doi.org/10.1055/s-2004-835850 PMID: 15643556

27. Vane JR, Botting RM. Anti-inflammatory drugs and their mechanism of action. Inflamm Res.1998; 47: S78–87. https://doi.org/10.1007/s000110050284 PMID: 9831328

28. Djerassi C, Gorman M, Nussbaum AL, Reynoso L. Alkaloid studies. IV. The isolation of reserpine, serpentine and ajmaline from *Rauwolfia heterophylla* Roem. and Schult. J Am Chem Soc.1954; 76:4463–4465

29. Dias DA, Urban S, Roessner U. A historical overview of natural products in drug discovery. Metabolites. 2012; 3: 303–336.

30. Lacy A, O'Kennedy R. Studies on coumarins and coumarin-related compounds to determine their therapeutic role in the treatment of cancer. Curr Pharm Des. 2004 10:3797–3811. https://doi.org/10.2174/1381612043382693 PMID: 15579072

31. Borges F, Roleira F, Milhazes N, Santana L, Uriarte E. Simple coumarins and analogues in medicinal chemistry: Occurrence, synthesis and biological activity. Curr Med Chem. 2005; 12: 887–916. https://doi.org/10.2174/0929867053507315 PMID: 15853704

32. Miadoková E. Isoflavonoids–An overview of their biological activities and potential health benefits. Interdiscip Toxicol. 2009; 2:211–218. https://doi.org/10.2478/v10102-009-0021-3 PMID: 21217857

33. Moss GP. Nomenclature of lignans and neolignans (IUPAC Recommendations 2000). Pure Appl Chem. 2000; 72:1493–1523.

34. Facchini PJ. Alkaloid biosynthesis in plants: Biochemistry, cell biology, molecular regulation, and metabolic engineering applications. Annu Rev Plant Physiol Plant Mol Biol. 2001; 52:29–66. https://doi.org/10.1146/annurev.arplant.52.1.29 PMID: 11337391

35. Ballatore C, Huryn DM, Smith AB III. Carboxylic acid (*bio*)isosteres in drug design. Chem Med Chem. 2013; 8: 385–395. https://doi.org/10.1002/cmdc.201200585 PMID: 23361977

36. Dutta S, Ray S, Nagarajan K. Glutamic acid as anticancer agent: An overview. Saudi Pharm J. 2013; 21: 337–343. https://doi.org/10.1016/j.jsps.2012.12.007 PMID: 24227952

37. Saarinen N, Mäkelä S, Santti R. Anticancer effects of lignans. In: Yagasaki K., Miura Y., Hatori M., Nomura Y.(eds), Animal Cell Technology: Basic & Applied Aspects, 2003; 13:55–58.

38. Mughal UR, Fatima I, Malik A, Tareen RB. Loasifolin, a new flavonoid from *Eremostachys loasifolia*. J Asian Nat Prod Res. 2010; 12: 328–330. https://doi.org/10.1080/10286021003627379 PMID: 20419544

39. Rauf A, Khan R, Muhammad N. Antioxidant studies of various solvent fractions and chemical constituents of *Potentilla evestita* Th. Wolf, Afr. J Pharm Pharmacol. 2013; 7: 2707–2710.

40. Faizi S, Dar A, Siddiqi H, Naqvi S, Naz A, Bano S, et al.,. Bioassay-guided isolation of antioxidant agents with analgesic properties from flowers of *Tagetes patula*. Pharm Biol. 2011; 49: 516–525. https://doi.org/10.3109/13880209.2010.523006 PMID: 21284510

41. Miftakhova AF, Burasheva GSh, Abilov ZhA, Ahmad VU, Zahid M. Coumarins from the aerial part of *Halocnemum strobilaceum*. Fitoterapia, 2001; 72:319–321. https://doi.org/10.1016/s0367-326x(00)00301-4 PMID: 11295318

42. Abbaskhan A, Choudhary MI, Ghayur MN, Parween Z, Shaheen F, Gilani AUH, et al.,. Biological Activities of Indian Celery, *Seseli diffusum* (Roxb. ex Sm.) Sant. & Wagh. Phytother Res. 2012; 26: 783–786. https://doi.org/10.1002/ptr.3600 PMID: 22095902

43. Tatuedom OK, Kouam SF, Yapna DB, Ngadjui BT, Green IR, Choudhary MI, et al.,. Spiroalkaloids and coumarins from the stem bark of *Pauridiantha callicarpoides*. Z Naturforsch. 2014; 69b: 747–752.

44. Shaheen F, Zeeshan M, Ahmad M, Anjum S, Ali S, Fun HK, et al., (2006). Norditerpenoid alkaloids from *Delphinium nordhagenii*. J Nat Prod. 2006; 69: 823–825. https://doi.org/10.1021/np050478m PMID: 16724850

45. Bera H, Dolzhenko AV, Sun L, Gupta SD, Chui W. Synthesis and *in vitro* evaluation of 1,2,4-triazolo [1,5-a][1,3,5]triazine derivatives as thymidine phosphorylase inhibitors. Chemical Biol Drug Des. 2013; 82: 351–360.

46. LigPrep, version 3.6, Schrödinger, LLC, New York, NY, 2015.

47. Protein Preparation Wizard 2015–4; Epik version 2.4, Schrödinger, LLC, New York, NY, 2015; Impact version 5.9, Schrödinger, LLC, New York, NY, 2015; Prime version 3.2, Schrödinger, LLC, New York, NY, 2015.

48. Sastry GM, Adzhigirey M, Day T, Annabhimoju R, Sherman WJ. Protein and ligand preparation: Parameters, protocols, and influence on virtual screening enrichments, Compute Aided Mol Des. 2013; 27: 221–234.

49. Halgren T. Identifying and characterizing binding sites and assessing druggability. J Chem Inf Model. 2009; 49:377–389. https://doi.org/10.1021/ci800324m PMID: 19434839

50. Schrödinger Release 2015–4: SiteMap, version 3.7, Schrödinger, LLC, New York, NY, 2015.

51. Glide, version 6.9, Schrödinger, LLC, New York, NY, 2015.

52. Friesner RA, Banks JL, Murphy RB, Halgren TA, Klicic JJ, Mainz DT, et al., Glide: A new approach for rapid, accurate docking and scoring. 1. Method and assessment of docking accuracy. J Med Chem. 2004; 47: 1739–1749. https://doi.org/10.1021/jm0306430 PMID: 15027865

53. Halgren TA, Murphy RB, Friesner RA, Beard HS, Frye LL, Pollard WT, et al., Glide: A new approach for rapid, accurate docking and scoring. 2. Chapter 1: Introduction 6 Schrödinger software release 2015–4 enrichment factors in database screening, J Med Chem. 2004; 47:1750–1759. https://doi.org/10.1021/jm030644s PMID: 15027866

54. Friesner RA, Murphy RB, Repasky MP, Frye LL, Greenwood JR, Halgren TA, et al.,. Extra precision glide: Docking and scoring incorporating a model of hydrophobic enclosure for protein-ligand complexes. J Med Chem. 2006; 49: 6177–6196. https://doi.org/10.1021/jm051256o PMID: 17034125

55. Prime, version 4.2, Schrödinger, LLC, New York, NY, 2015.

56. Dimas K, Demetzos C, Marsellos M, Stiriadou R, Malamas M, Kokkinopoulos D. Cytotoxic activity of labdane type diterpenes against human leukemia cell lines *in vitro*. Planta Med. 1997; 64: 208–211.

57. Khan JA, Javaid S, Maryam AG, Huwait E, Shaikh M, Shafqat A, et al., (2017). Studies on new urease inhibitors by using biochemical, STD-NMR spectroscopy, and molecular docking methods. Med Chem Res. 2017; 26: 2452–2467.